

Folding a Nonbiological Polymer into a Compact Multihelical Structure

Byoung-Chul Lee,[†] Ronald N. Zuckermann,^{*,§} and Ken A. Dill^{*,†,‡}

Contribution from the Graduate Group in Biophysics and Department of Pharmaceutical Chemistry, University of California, 600 16th Street, San Francisco, California 94143, and Chiron Corporation, 4560 Horton Street, Emeryville, California 94608

Received March 8, 2005; E-mail: dill@maxwell.compbio.ucsf.edu; ron_zuckermann@chiron.com

Abstract: The only molecules that are currently known to fold into unique three-dimensional conformations and perform sophisticated functions are biological polymers – proteins and some RNA molecules. Our aim is to create a nonbiological sequence-specific polymer that folds in aqueous solution. Toward that end, we synthesized sequence-specific 30mer, 45mer, and 60mer peptoid oligomers (N-substituted glycine polymers) consisting of 15mer units we chained together by disulfide and oxime linkages to mimic the helical bundle structures commonly found in proteins. Because these 15mer sequences were previously shown to form defined helical structures that aggregate together at submillimolar concentrations, we expected that by covalently linking multiple 15mers together, they might fold as helical bundles. To probe whether they folded, we used fluorescence resonance energy transfer (FRET) reporter groups. We found that certain constructs fold up with a hydrophobic core and have cooperative folding transitions. Such molecules may ultimately provide a platform for designing specific functions resembling those of proteins.

Introduction

Proteins perform biological functions. No synthetic polymer currently has the capacity to perform such sophisticated functions, such as specific molecular recognition, catalysis, transport, energy conversion, etc. Why not? One view holds that proteins are unique because of their monomer set, the amino acids. However, that is unlikely because some RNA molecules are also functional. Another view says that the essence of biological function is in the ability to fold, and the essence of folding is in biology's ability to synthesize specific sequences of monomer units that follow a hydrophobic/polar code.¹ This view follows from statistical mechanical modeling, which has shown that polymers having particular sequences of hydrophobic and polar monomers should be able to fold uniquely.¹ Our aim is to test that hypothesis, using nonbiological oligomers to try to create foldable molecules with defined tertiary structures in aqueous solution.

In support of this hypothesis, there is evidence that the hydrophobic and polar patterning of a sequence in polypeptide molecules is sufficient to produce a stable tertiary structure with a well-defined hydrophobic core.² Moreover, proteins can fold even when using a small alphabet of hydrophobic and polar residues.³

There have been recent efforts to construct synthetic polymers that mimic protein properties.⁴ Yet, it has been difficult to achieve stable secondary structures, a multi-letter alphabet, and long chain lengths within a single type of polymer. A wide variety of synthetic polymers have been developed to overcome many of these hurdles. For example, β -peptides, anthranilamide oligomers, and oligo(*m*-phenylene ethynylene) have been shown to form stable helices.^{5–7} Oligourea, oligopyrrolinones, and azatides also mimic protein secondary structures, but are currently limited to relatively short chain-lengths.^{8–10} No nativelike tertiary structures have yet been reported in synthetic heteropolymers, although researchers are making progress.^{11,12}

[†] Graduate Group in Biophysics, University of California.

[‡] Department of Pharmaceutical Chemistry, University of California.

[§] Chiron Corp.

(1) (a) Lau, K. F.; Dill, K. A. *Macromolecules* **1989**, *22*, 3986–3997. (b) Shakhnovich, E. I.; Gutin, A. M. *Nature* **1990**, *346*, 773–775. (c) Leopold, P. E.; Montal, M.; Onuchic, J. N. *Proc. Natl. Acad. Sci. U.S.A.* **1992**, *89*, 8721–8725. (d) Sali, A.; Shakhnovich, E.; Karplus, M. *J. Mol. Biol.* **1994**, *235*, 1614–1636. (e) Li, H.; Helling, R.; Tang, C.; Wingreen, N. *Science* **1996**, *273*, 666–669. (f) Chan, H. S.; Dill, K. A. *Annu. Rev. Biophys. Chem.* **1991**, *20*, 447–490. (g) Onuchic, J. N.; Luthey-Schulten, Z.; Wolynes, P. G. *Annu. Rev. Phys. Chem.* **1997**, *48*, 545–600.

(2) (a) Kamtekar, S.; Schiffer, J. M.; Xiong, H.; Babik, J. M.; Hecht, M. H. *Science* **1993**, *262*, 1680–1685. (b) Wei, Y.; Kim, S.; Fela, D.; Baum, J.; Hecht, M. H. *Proc. Natl. Acad. Sci. U.S.A.* **2003**, *100*, 13270–13273. (3) (a) Riddle, D. S.; Santiago, J. V.; Bray-Hall, S. T.; Doshi, N.; Grantcharova, V. P.; Yi, Q.; Baker, D. *Nat. Struct. Biol.* **1997**, *10*, 805–809. (b) Bowie, J. U.; Reidhaar-Olson, J. F.; Lim, W. A.; Sauer, R. T. *Science* **1990**, *247*, 1306–1310. (4) (a) Hill, D. J.; Mio, M. J.; Prince, R. B.; Hughes, T. S.; Moore, J. S. *Chem. Rev.* **2001**, *101*, 3893–4012. (b) Kirshenbaum, K.; Zuckermann, R. N.; Dill, K. A. *Curr. Opin. Struct. Biol.* **1999**, *9*, 530–535. (5) Cheng, R. P.; Gellman, S. H.; DeGrado, W. F. *Chem. Rev.* **2001**, *101*, 3219–3232. (6) (a) Hamuro, Y.; Geib, S. J.; Hamilton, A. D. *J. Am. Chem. Soc.* **1996**, *118*, 7529–7541. (b) Hamuro, Y.; Geib, S. J.; Hamilton, A. D. *J. Am. Chem. Soc.* **1997**, *119*, 10587–10593. (7) Nelson, J. C.; Saven, J. G.; Moore, J. S.; Wolynes, P. G. *Science* **1997**, *277*, 1793–1796. (8) (a) Nowick, J. S.; Powell, N. A.; Nguyen, T. M.; Noronha, G. *J. Org. Chem.* **1992**, *57*, 3763–3765. (b) Nowick, J. S.; Mahrus, S.; Smith, E. M.; Ziller, J. W. *J. Am. Chem. Soc.* **1996**, *118*, 2764–2765. (9) Smith, A. B., III; Guzman, M. C.; Sprengeler, P. A.; Keenan, T. P.; Holcomb, R. C.; Wood, J. L.; Hirschmann, R. J. *J. Am. Chem. Soc.* **1994**, *116*, 9947–9962. (10) Han, J.; Janda, K. D. *J. Am. Chem. Soc.* **1996**, *118*, 2539–2544. (11) (a) Raguse, T. L.; Lai, J. R.; LePlae, P. R.; Gellman, S. H. *Org. Lett.* **2001**, *3*, 3963–3966. (b) Cheng, R. P.; DeGrado, W. F. *J. Am. Chem. Soc.* **2002**, *124*, 11564–11565.

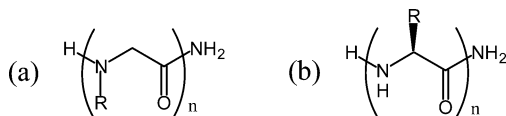


Figure 1. (a) Peptoid, or N-substituted glycine oligomer. (b) Peptide, for comparison.

However, the recent invention of peptoid polymers has opened up the opportunity for synthesizing relatively long specific sequences that utilize a wide array of possible monomers.¹³ Peptoids are N-substituted glycine oligomers in which the side-chains are appended to the backbone nitrogen (Figure 1).

The N-substitution in peptoids precludes the kind of intra-backbone hydrogen bonding that is found in proteins. However, this presents us the opportunity to explore whether tertiary structure can be formed in the absence of backbone hydrogen bonding. In terms of sequence diversity, over 300 primary amines are currently available that can be incorporated into peptoids as side-chains. Peptoids are efficiently synthesized using the solid-phase submonomer method, which consists of a two-step monomer addition cycle involving bromoacylation and subsequent nucleophilic displacement by primary amines.¹⁴ Using this method, we have synthesized peptoids up to 48mers in reasonable yields.¹⁵ Peptoids as short as 5mers have been shown to adopt helical conformations when they contain chiral side-chains adjacent to the main chain nitrogen.¹⁶ 2D-NMR and X-ray crystallographic studies of pentameric peptoids that showed helices contain 3 residues per turn and have a pitch of roughly 6.0–6.7 Å, respectively.^{17,18} The helix-inducing property of chiral side-chains has also been seen in computational modeling.¹⁹

Our aim was to design the simplest possible tertiary structure, a helical bundle based on amphiphilic helices. Interesting functions (e.g., heme binding) have previously been encoded into helix bundle folds made from both synthetic and biologically expressed peptides.²⁰ Based on our previous finding that amphiphilic peptoid 15mers noncovalently associate into helical multimers at submillimolar concentrations in aqueous solution,¹² we decided here to covalently link such 15mers together, to see if they would adopt a tertiary structure. We previously screened for 1-anilinonaphthalene 8-sulfonate (1,8-ANS) fluorescence from a library of more than 3000 amphiphilic helices of peptoid 15mers.¹² A small number of sequences were found

that caused a large fluorescent signal of ANS, and these were subsequently shown to associate into helical multimers. We chose one of the amphiphilic helical 15mers (see Figure 2) for our study that self-assembles into a trimer at submillimolar concentrations in aqueous solution.

In light of the challenge of total synthesis of a single-chain long peptoid, we preferred instead to couple helical 15mer segments together (Figure 3). The coupling between peptide segments has been used for the synthesis of long polypeptides.²¹ Thus, the chemical conjugation between the helices should provide a significant step toward the synthesis of an artificial protein.

Results and Discussion

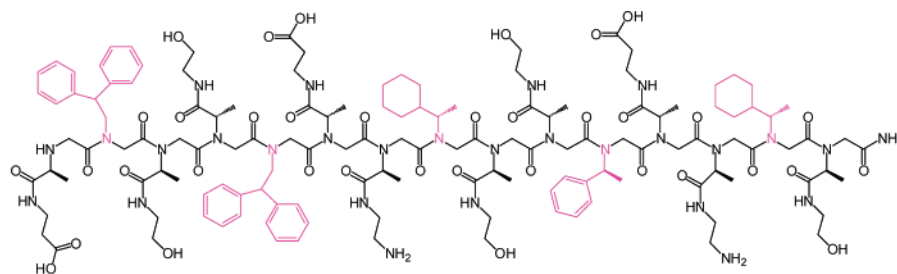
Synthesis of Peptoid Single-Chain Helix Bundles. The chemical synthesis of a single-chain four-helix bundle presents a major technical hurdle. For a peptoid four-helix bundle, having more than 60 monomers, a coupling yield for each submonomer cycle must be greater than 99% to obtain a 55% yield of the final product. In general, the peptoid monomer addition cycle results in >99% yields. However, the incorporation of complex side-chains such as Nsahe, Nsace, and Nsaae (Table 1) can slightly reduce this yield, although we optimized the acylation step of the submonomer cycle by reducing the amount of the bromoacetic acid and changing the ratio of diisopropylcarbodiimide (DIC):bromoacetic acid (0.93:1) (Experimental Section). For this reason, we used chemical conjugation to link helical units together. Chemical conjugation also allows for the combinatorial ligation of a variety of helical 15mer analogues (with either head-to-head or head-to-tail orientations). To conjugate pairs of peptoid helices, we used disulfide linkages (prepared from a sulfhydryl group and an activated disulfide) and oxime linkages (prepared from aldehyde and aminoxy groups) (Figure 4). We previously described the incorporation of these chemoselective groups into peptoids. Ligation reactions using these groups occur in high yield and are orthogonal to side-chain functionalities.²²

To conjugate two peptoids, we used a disulfide linkage. Peptoid units with a sulfhydryl (U^1 and U^3 in Figure 4a) and an activated disulfide group (U^4 in Figure 4a) were each purified and then ligated together at pH 7. The ligation reaction via disulfide formation gave a yield of ~60%, and the product conjugates were further purified to more than 95% purity (Supporting Information). Tail-to-head ($U^1 + U^4$; **8**, **9**, **10**, **11**, **12**, **15**, **16**, **19**, and **20**) and head-to-head ($U^3 + U^4$; **13**, **14**, **17**, and **18**) orientations of peptoid conjugates were also generated (Figure 6).

To conjugate three peptoids, we used one oxime and one disulfide linkage. To conjugate four peptoids, we used one oxime and two disulfide linkages (Figure 4). For the conjugation of three and four helices, two ligating groups were incorporated into the internal peptoid units U^5 and U^6 – one at each terminus – (Figure 4a) to ligate other peptoids at each end. Peptoid unit U^5 has an activated disulfide and an aldehyde at the N- and C-terminus, respectively. Peptoid unit U^6 has an aminoxy and

- (12) Burkoth, T. S.; Beausoleil, E.; Kaur, S.; Tang, D.; Cohen, F. E.; Zuckermann, R. N. *Chem. Biol.* **2002**, *9*, 647–654.
 (13) Patch, J. A.; Kirshenbaum, K.; Seuryneck, S. L.; Zuckermann, R. N.; Barron, A. E. I. Versatile oligo(N-substituted) glycines: the many roles of peptoids in drug discovery. In *Pseudo-Peptides in Drug Discovery*; Nielsen, P. E., Ed.; Wiley-VCH: Weinheim, 2004; p 1.
 (14) Zuckermann, R. N.; Kerr, J. M.; Kent, S. B. H.; Moos, W. H. *J. Am. Chem. Soc.* **1992**, *114*, 10646–10647.
 (15) Murphy, J. E.; Uno, T.; Hamer, J. D.; Cohen, F. E.; Dwarki, V.; Zuckermann, R. N. *Proc. Natl. Acad. Sci. U.S.A.* **1998**, *95*, 1517–1522.
 (16) Kirshenbaum, K.; Barron, A. E.; Goldsmith, R. A.; Armand, P.; Bradley, E. K.; Truong, K. T.; Dill, K. A.; Cohen, F. E.; Zuckermann, R. N. *Proc. Natl. Acad. Sci. U.S.A.* **1998**, *95*, 4303–4308.
 (17) Armand, P.; Kirshenbaum, K.; Goldsmith, R. A.; Farr-Jones, S.; Barron, A. E.; Truong, K. T.; Dill, K. A.; Mierke, D. F.; Cohen, F. E.; Zuckermann, R. N.; Bradley, E. K. *Proc. Natl. Acad. Sci. U.S.A.* **1998**, *95*, 4309–4314.
 (18) Wu, C. W.; Kirshenbaum, K.; Sanborn, T. J.; Patch, J. A.; Huang, K.; Dill, K. A.; Zuckermann, R. N.; Barron, A. E. *J. Am. Chem. Soc.* **2003**, *125*, 13525–13530.
 (19) Armand, P.; Kirshenbaum, K.; Falicov, A.; Dunbrack, R. L., Jr.; Dill, K. A.; Zuckermann, R. N.; Cohen, F. E. *Fold. Des.* **1997**, *2*, 369–375.
 (20) (a) Choma, C. T.; Lear, J. D.; Nelson, M. J.; Dutton, P. L.; Robertson, D. E.; DeGrado, W. F. *J. Am. Chem. Soc.* **1994**, *116*, 856–865. (b) Rojas, N. R.; Kamtekar, S.; Simons, C. T.; McLean, J. E.; Vogel, K. M.; Spiro, T. G.; Farid, R. S.; Hecht, M. H. *Protein Sci.* **1997**, *6*, 2512–2524.

- (21) (a) Muir, T. W. *Annu. Rev. Biochem.* **2003**, *72*, 249–289. (b) Dawson, P. E.; Kent, S. B. *Annu. Rev. Biochem.* **2000**, *69*, 923–960. (c) Nilsson, B. L.; Soellner, M. B.; Raines, R. T. *Annu. Rev. Biophys. Biomol. Struct.* **2004**, *34*, 91–118.
 (22) Horn, T.; Lee, B.-C.; Dill, K. A.; Zuckermann, R. N. *Bioconjugate Chem.* **2004**, *15*, 428–435.



(N) - Nsace N α pe Nsahe Nsahe N α pe Nsace Nsaae Nsch Nsahe Nsahe Nspe Nsace Nsaae Nsch Nsahe - (C)

Figure 2. The chemical structure and sequence of the amphiphilic helical 15mer chosen from the previous study.¹² This sequence was modified at the N- and C-termini and joined via chemical conjugation to create peptoid helix bundles. See Table 1 for the abbreviations of side-chains. Nonpolar side-chains are colored violet.

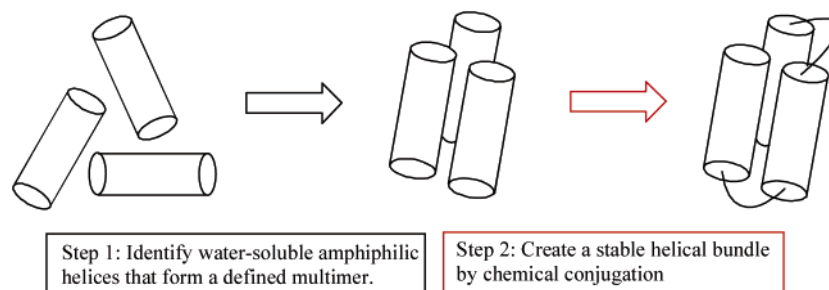


Figure 3. Creation of a three-dimensional fold by the chemical conjugation of helical peptoids. Amphiphilic helical peptoid 15mers were screened previously by looking at ANS fluorescence (step 1). Those sequences formed a multimer at submillimolar concentrations. Our aim is to create a single-chain helical bundle by the chemical conjugation of those helical peptoids together (step 2).

a sulfhydryl group at the N- and C-terminus, respectively. For the synthesis of the three-peptoid conjugates (**21**, **22**, and **23**), units U^4 and U^6 were first ligated with a disulfide bond and purified ($U^4 + U^6$ in Figure 5a). Peptoid unit U^2 was then combined with conjugate $U^4 + U^6$ to form an oxime bond to generate the final product in $\sim 40\%$ yield. The three-peptoid conjugates were then purified to $>95\%$ purity. For example, HPLC profiles are shown in Figure 5a for the synthesis of one of the three-peptoid conjugates, peptoid **21**. The mass spectrum of the peptoid **21** showed the expected charged peaks (Figure 5b). For the conjugation of four peptoids (**24** and **25**), unit U^1 and U^5 , and unit U^4 and U^6 were first ligated and purified to generate the two-peptoid conjugates with a disulfide bond. Next, both of them were mixed together to generate the four-peptoid conjugate with an oxime bond ($\sim 40\%$ yield) and purified further to more than 90% purity (Supporting Information).

The HPLC reaction profiles and mass spectra for other peptoid conjugates are shown in the Supporting Information. The chemical structure and abbreviations of side-chains, and detailed sequences of the 25 peptoids used in our study, are shown in Table 1 and Figure 6, respectively. Summarized in Table 2 are the molecular weights of the peptoids as determined by mass spectrometry.

Our naming scheme for peptoids is as follows. The first part of the name is the number of monomers; followed by Chi for chiral residues, Ach for achiral residues, or Pel for polyelectrolyte peptoids; then we indicate the configuration of the helix orientation (CN for tail to head and NN for head to head ligation); followed by an indication about a possible FRET pair (FQ for fluorescence donor and quencher at both ends of chain and F for fluorescence donor only at one end).

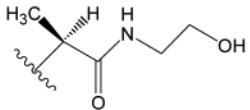
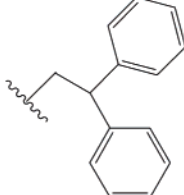
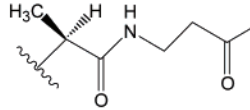
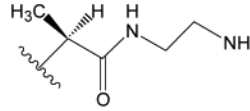
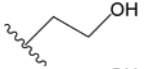
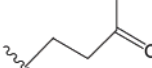
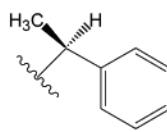
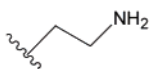
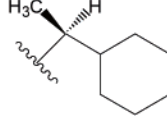
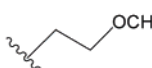
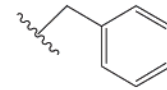
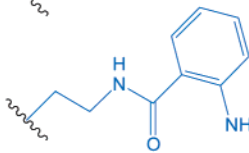
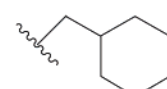
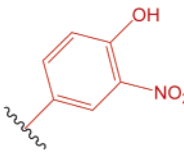
Design and Synthesis of Two-Peptoid Conjugates. In this study, we linked two amphiphilic helical peptoid 15mers

together (Figure 2). In addition, we synthesized other peptoid sequences of two-peptoid conjugates to test the effects of side-chain chirality, periodicity of nonpolar groups, and the helix orientation on the putative tertiary structure. Our archetypical peptoid 15mer has chiral side-chains, and nonpolar groups repeat at every third residue (Figure 2). It has been shown previously that chirality at the N, α position of the majority of side-chains is critical for the formation of helical secondary structures.¹⁶ To explore the effect of side-chain chirality on the compactness of the tertiary structure, we synthesized 30mer peptoids with entirely achiral side-chains (**15–18**), while maintaining the pattern of nonpolar groups. Two different helix orientations (tail to head peptoids **10–12**, **15**, and **16**; head to head peptoids **13**, **14**, **17**, and **18**) were tested to see which orientation is optimal for the structural compactness. To test the effects of nonpolar group periodicity, we synthesized control peptoid 22mers (**8** and **9**) with nonpolar groups incorporated into the peptoid at every second sequence position. The sequences of these peptoids are not the same length with other two-peptoid conjugates (30mers), but were designed to have the same number of nonpolar groups as the peptoid 30mer **10**. As an additional control, to create a peptoid without a hydrophobic core, we synthesized polyelectrolyte 30mers (**19** and **20**) that contain alternating methoxyethyl and aminoethyl groups.

To test whether our peptoids fold into a compact structure, we put a fluorescence donor (anthranilamide) on one end of the putative 2-helix bundle and a quencher (amino-nitrophenol) on the other as fluorescence resonance energy transfer (FRET) reporter groups.²³ FRET measures the distance between the donor and acceptor in a molecule.²⁴ As a reference for measuring the FRET efficiency, we synthesized peptoids having

(23) Mezo, A. R.; Cheng, R. P.; Imperiali, B. *J. Am. Chem. Soc.* **2001**, *123*, 3885–3891.

Table 1. Side-Chains Used in Our Study (Fluorescent Donor and Quencher Are Colored Blue and Red, Respectively)

| | | | |
|--|--|---|---|
|  | (S)-N-(N'-2-hydroxyethyl alaninamide) glycine Nsae |  | N-(1-diphenylethyl) glycine Ndpe |
|  | (S)-N-(N'-2-carboxymethyl alaninamide) glycine Nsace | | |
|  | (S)-N-(N'-2-aminoethyl alaninamide) glycine Nsaee |  | N-(2-hydroxyethyl) glycine Nser |
| | |  | N-(2-carboxylethyl) glycine Nglu |
|  | (S)-N-(1-phenylethyl) glycine Nspe |  | N-(2-aminoethyl) glycine Nae |
|  | (S)-N-(1-cyclohexylethyl) glycine Nsch |  | N-(methoxyethyl) glycine Nme |
|  | N-(1-phenylmethyl) glycine Npm |  | N-(2-anthranilamido-ethyl) glycine Naae |
|  | N-(1-cyclohexylmethyl) glycine Nchm |  | N-(2-nitrophenol) glycine Nnp |

identical sequences but with only a fluorescence donor, and no quencher. To incorporate the fluorescence donor into the peptoid as a side-chain, we synthesized the primary amine derivative of anthranilamide. The quencher (amino-nitrophenol) is commercially available and can be incorporated itself into peptoid as a submonomer during peptoid synthesis. We determined the effective distance R_0 of the FRET pair to be 31 Å. This is the distance at which half the donor fluorescence is quenched (see Experimental Section). This suggests that the FRET pair should be useful for measuring distances in a range suitable for our studies (19–51 Å for a FRET efficiency of 0.95–0.05). It is expected that the donor fluorescence should be strongly quenched in the folded state where the donor fluorophore and the quencher are brought together in close proximity (Figure 7). In control compounds where these two groups are covalently constrained to be close to one another (**1**; 5_FQ_1), or separated by one and two residues (**2**; 5_FQ_2, and **3**; 5_FQ_3), donor fluorescence is strongly quenched with a FRET efficiency more than 0.98, as expected (Supporting Information). A free fluorophore analogue (amino-methylbenzamide) in solution is not quenched by a free quencher (amino-nitrophenol) at a concentration of 2 μM, the same as that of peptoids used here (Supporting Information), suggesting that the FRET pair of anthranilamide and amino-nitrophenol must be held close together for efficient quenching.

All of the peptoids that we designed to fold, that is, those having nonpolar groups every third residue, showed FRET efficiencies of 0.84–0.87 at pH 7 in the absence of denaturant (Figure 8a and Figure 10a). These values correspond to a distance of ~22 Å.

Folding Cooperativity of Peptoid Two-Helix Bundle. We studied the folding cooperativity of each peptoid by denaturant equilibrium titration. Guanidine hydrochloride (GdnHCl), a denaturant commonly used in protein unfolding, did not appear to unfold peptoids cooperatively (Supporting Information). Guanidine is believed to destabilize proteins through both hydrophobic and hydrogen-bonding interactions. We believe that the ineffectiveness of guanidine in peptoid unfolding is because peptoids have no intra-backbone hydrogen bonding.

We believe that the compact multihelical structures we observe here are driven by hydrophobic interactions. The unfolding transition is cooperatively induced in the presence of a hydrophobic solvent, acetonitrile (Figure 8). Cooperativity does not appear to be due to aggregation. For a 30mer peptoid (**10**; 30_Chi_CN_FQ), the titration profiles are independent of the peptoid concentrations over a 10-fold range from 0.5 to 5 μM. Analytical gel filtration of the peptoid indicated that the peptoid migrates as a monomer (Supporting Information). A further indication that hydrophobic forces predominate is that cooperative unfolding occurs in all of the 30mers that contain hydrophobic groups at every third residue (Figure 8). In contrast, the random-coil polyelectrolyte (**19**; 30_Pel_CN_FQ) and the

(24) Zhang, J.; Tamilarasu, N.; Hwang, S.; Garber, M. E.; Huq, I.; Jones, K. A.; Rana, T. M. *J. Biol. Chem.* **2000**, *275*, 34314–34319.

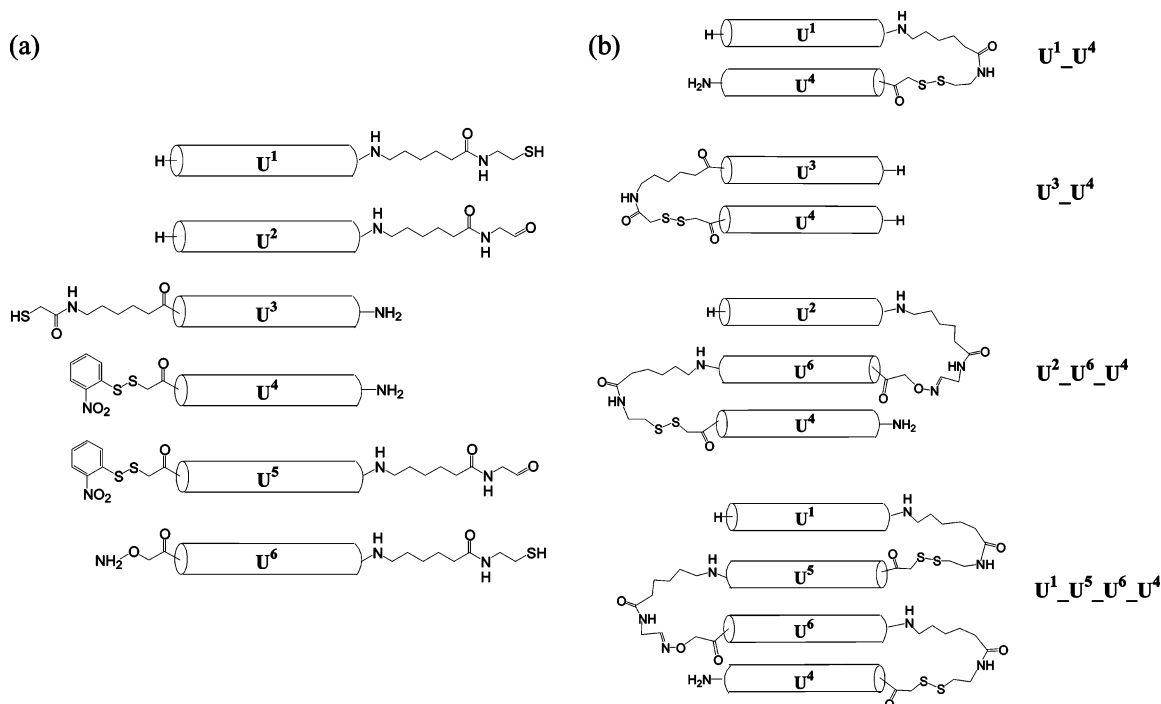


Figure 4. Chemoselective ligation between peptoids. (a) Various peptoid units with ligation groups. Units U¹ and U² have a sulfhydryl and aldehyde group at the C-terminus, respectively. Units U³ and U⁴ have a sulfhydryl and activated disulfide group at the N-terminus, respectively. Unit U⁵ has both an N-terminal activated disulfide and a C-terminal aldehyde group. Unit U⁶ has both an N-terminal aminoxy and a C-terminal sulfhydryl group. (b) The chemical conjugation between peptoid units. For two-peptoid conjugates, tail to head (U¹ + U⁴) and head to head (U³ + U⁴) orientations were generated by mixing two peptoids. For three-peptoid conjugates, U⁴, U⁶, and U² were used. Units U⁴ and U⁶ were first mixed to generate a two-peptoid conjugate with disulfide bond. Next, unit U² was ligated onto the two-peptoid conjugate with an oxime bond between aminoxy group at N-terminus of unit U⁶ and aldehyde group at the C-terminus of unit U². For four-peptoid conjugates, two of the two-peptoid conjugates (U⁴ + U⁶ and U¹ + U⁵) were ligated via an oxime linkage.

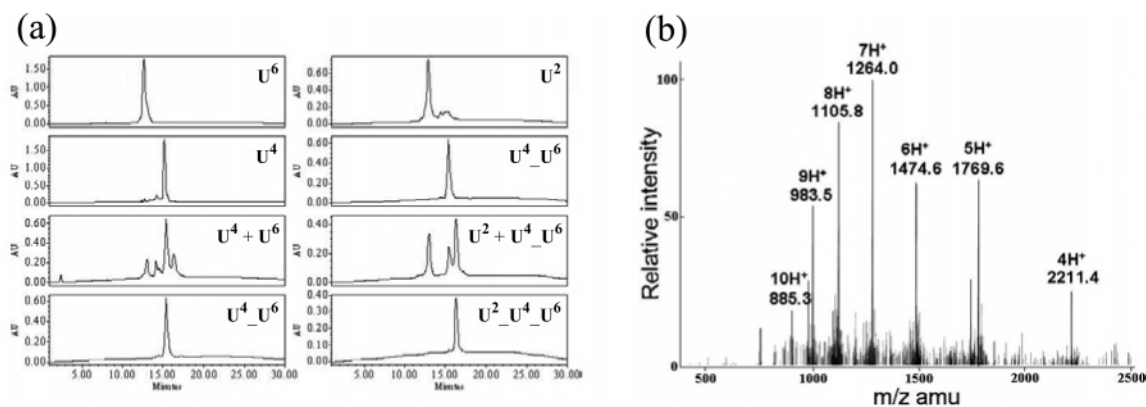


Figure 5. Synthesis of peptoid 45mer, **21** (45_Chi_CN_FQ). (a) HPLC profiles of the peptoid conjugation. Units U⁶ and U⁴ were first ligated to form a two-peptoid conjugate U⁴-U⁶. Next, unit U² was combined with the U⁴-U⁶ to generate the peptoid **21** (45_Chi_CN_FQ) (U²-U⁴-U⁶). (b) Mass spectrum of the final product of the three-peptoid conjugate **21** (45_Chi_CN_FQ).

alternating periodicity control peptoid (**8**; 22_Chi_CN_FQ) in which nonpolar groups are incorporated at every second residue do not show cooperative unfolding (Figure 8).

We fitted the folding transition data shown in Figures 8a, 9, and 10a to a two-state model (Experimental Section). This gives the thermodynamic stability (ΔG_u (H₂O)) at zero denaturant, and a folding cooperativity (m value, the denaturant dependence of folding free energy ΔG_u). The m value typically correlates with the change in solvent accessible area between folded and unfolded states.²⁵ Hence, larger m values imply more hydrophobic burial within a folded state.

All of the 30mers that showed a cooperative unfolding transition in acetonitrile:water have similar values of ΔG_u (H₂O), but differ in their m values, depending on the chirality of the

side-chains (Table 3). The m value is not affected by the orientation of the two helical segments in 30mers (head to tail or head to head). Peptoids with achiral side-chains have a greater m value than peptoids with chiral side-chains, suggesting that peptoids with achiral side-chains bury more hydrophobic surface inside a folded state. The achiral side-chains in peptoids might give a more flexible backbone than chiral side-chains, yielding a tighter packing of hydrophobic groups.

However, the secondary structure is more pronounced in peptoids with chiral side-chains (**10**; 30_Chi_CN_FQ and **13**; 30_Chi_NN_FQ) than in other 30mers, based on far-UV CD spectra of 30mers (Figure 8b). Peptoids with achiral side-chains

(25) Myers, J. K.; Pace, C. N.; Scholtz, J. M. *Protein Sci.* **1995**, *4*, 2138–2148.

Table 2. Molecular Weight of Each Peptoid Found from Mass Spectrometry

| peptoid | oligomer length | molecular weight (calc.:found) |
|----------------------------|-----------------|--------------------------------|
| 1 (5_FQ_1) | 5 | 775.8:775.8 |
| 2 (5_FQ_2) | 5 | 775.8:775.8 |
| 3 (5_FQ_3) | 5 | 775.8:775.8 |
| 4 (5_F) | 5 | 696.8:696.9 |
| 5 (15_Chi_FQ) | 15 | 2832.2:2832.0 |
| 6 (15_Chi_F) | 15 | 2810.3:2811.8 |
| 7 (15_Chi) | 15 | 2791.2:2791.1 |
| 8 (22_Chi_CN_FQ) | 22 | 4490.3:4492.5 |
| 9 (22_Chi_CN_F) | 22 | 4496.4:4499.0 |
| 10 (30_Chi_CN_FQ) | 30 | 5868.8:5867.4 |
| 11 (30_Chi_CN_F) | 30 | 5846.8:5847.1 |
| 12 (30_Chi_CN) | 30 | 5827.8:5827.1 |
| 13 (30_Chi_NN_FQ) | 30 | 5910.8:5909.9 |
| 14 (30_Chi_NN_F) | 30 | 5887.8:5887.6 |
| 15 (30_Ach_CN_FQ) | 30 | 4505.2:4505.0 |
| 16 (30_Ach_CN_F) | 30 | 4412.2:4412.3 |
| 17 (30_Ach_NN_FQ) | 30 | 4547.2:4546.5 |
| 18 (30_Ach_NN_F) | 30 | 4454.2:4453.2 |
| 19 (30_Pel_CN_FQ) | 30 | 3706.3:3708.0 |
| 20 (30_Pel_CN_F) | 30 | 3612.3:3613.9 |
| 21 (45_Chi_CN_FQ) | 45 | 8842.2:8841.4 |
| 22 (45_Chi_CN_FQ_2) | 45 | 8870.2:8869.5 |
| 23 (45_Chi_CN_F) | 45 | 8848.3:8849.3 |
| 24 (60_Chi_CN_FQ) | 60 | 11 906.8:11 906.1 |
| 25 (60_Chi_CN_F) | 60 | 11 884.8:11 884.8 |

(**15**; 30_Ach_CN_FQ and **17**; 30_Ach_NN_FQ) have featureless CD spectra at far-UV region.

In some of our peptoids, we disrupted the 3-unit sequence pattern, and had alternating hydrophobic/polar monomers instead (**8**; 22_Chi_CN_FQ). For these molecules, the CD spectrum at 222 nm is weaker than that of the original helical peptoid (Figure 8b). The overall shape of the spectrum for the peptoid **8** (22_Chi_CN_FQ) indicates a mixture of random-coil (negative CD around 195 nm) and secondary structure (weaker CD around 220 nm than that of helix). The peptoid **8** (22_Chi_CN_FQ) lacks a well-defined hydrophobic core: we see no cooperative unfolding transition induced by acetonitrile (Figure 8a). Our data are consistent with the hypothesis that chiral side-chains induce a helical secondary structure having three residues per turn.^{17–19} The backbone carbonyl group of peptoids is sterically hindered by the bulky group at the N, β position of the side-chain at the same residue, yielding a strong preference of negative backbone ϕ angle and a “polyproline type I”-like helical structure with three residues per turn.¹⁹ When nonpolar groups in a peptoid repeat at every third residue, it creates an amphipathic helix, with a stripe of hydrophobics on one side. However, the periodicity of nonpolar groups at every two residues affects the geometrical constraints imposed by chirality of side-chain as indicated by the far-UV spectrum (Figure 8b). This suggests that the hydrophobic interactions in the peptoid **8** (22_Chi_CN_FQ) struggle against the geometrical constraints.

Various water-miscible organic solvents also induced a cooperative melting of the peptoid (Figure 9a). A quantitative test of hydrophobic cores in proteins is to denature them using a series of increasingly hydrophobic alcohols.²⁶ Sometimes the strength of intra-backbone hydrogen bonding becomes stronger in organic solvents and stabilizes the protein, giving ambiguity in interpretation of the experimental results.²⁷ In the case of

peptoids, because we have no backbone hydrogen bonding, this artifact is not possible. As we increased the alcohol hydrophobicity, the degree of denaturation increased as well (Figure 9a). The magnitude and sharpness of these unfolding transitions with a series of alcohols is comparable to that of proteins including cytochrome C, α -chymotrypsinogen, myoglobin, etc.²⁶ The m value increases at longer alkyl chains of alcohol (Figure 9d and Table 3), suggesting that the main stabilizing force in the folding core of the 30mer peptoids is a hydrophobic interaction.

Peptoids with chiral side-chains still maintain secondary structure at high concentration of acetonitrile where the tertiary structure of peptoids is disrupted, based upon the CD signals of peptoids **7** (15_Chi) and **10** (30_Chi_CN_FQ) at \sim 12 M acetonitrile (Supporting Information). Acetonitrile does not break up the helical secondary structure induced by the chirality of the side-chains. The acetonitrile only melts the long-range hydrophobic contacts of the peptoid. Thus, it is suggested that the docking of preexisting helical units of the peptoid by inter-helical hydrophobic interactions is responsible for the folding of peptoid helix bundles.

Chain-Length Dependence of Folding Cooperativity. In general, we expect that longer chains should fold with greater stability. To determine nonpolar burial, we measured ΔG_u (H₂O) and m values of different chain lengths of peptoids by acetonitrile equilibrium titration. Analytical gel filtration of these peptoids (**10**; 30_Chi_CN_FQ, **21**; 45_Chi_CN_FQ, and **24**; 60_Chi_CN_FQ) indicated that they migrate as a monomer (Supporting Information). Thus, the cooperative transition induced by acetonitrile is due to the unfolding of hydrophobic core and not aggregation. ΔG_u (H₂O) and the m value increase when the chain-length of the peptoid increases up to the putative three-helix bundle 45mer (**21**; 45_Chi_CN_FQ), indicating that more hydrophobic groups are buried inside and that those hydrophobic cores are more stable (Figure 10 and Table 3). When using a series of alcohols, a similar propensity was observed (Figure 9 and Table 3). More hydrophobic alcohols are more potent for the unfolding of these peptoids as indicated by the m value (Figure 9d and Table 3).

However, when four helical units are conjugated together (**24**; 60_Chi_CN_FQ), the hydrophobic core is less stable than that of the 45mer. ΔG_u (H₂O) and the m value of the 60mer (**24**; 60_Chi_CN_FQ) are less than those of the three-helix bundle peptoid (**21**; 45_Chi_CN_FQ) and similar to those of the putative two-helix bundle peptoid (**10**; 30_Chi_CN_FQ) (Table 3). Thus, the three-helix bundle is the most optimized structure that the 15mer helical unit can coordinate. This result agrees with previous data of the unlinked 15mer helical peptoid that showed the formation of trimer at submillimolar concentration.¹² Further evidence that the 3-helix bundle is the most compact is seen from the size-exclusion chromatography retention times, which shows the 3-helix bundle eluting significantly faster than expected (see Supporting Information). We conclude that, among the possible helix bundles constructed from this 15-mer, the 3-helix bundle is the most stable. Single-domain proteins of approximately 60 residues in length have a ΔG_u (H₂O) in the range of 2–8 kcal/mol.²⁸ Thus, the stability of the putative three-helix peptoid is comparable to that of similar size of protein.

(26) Herskovits, T. T.; Gadegbeku, B.; Jailliet, H. *J. Biol. Chem.* **1970**, *245*, 2588–2598.

(27) Tanford, C. *Adv. Protein Chem.* **1968**, *23*, 121–282.

(28) Fulton, K. F.; Devlin, G. L.; Jodun, R. A.; Silvestri, L.; Bottomley, S. P.; Fersht, A. R.; Buckle, A. M. *Nucleic Acids Res.* **2005**, *33*, D279–283.

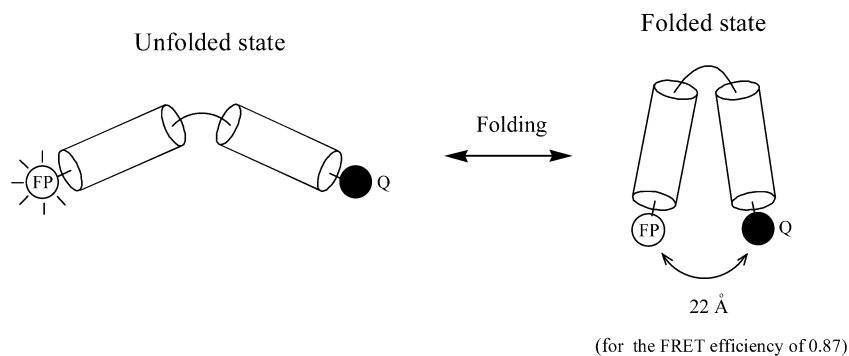


Figure 7. Schematic diagram of the FRET probes used in our study. It is expected that fluorescence donor and quencher are brought together in the folded state to quench the donor fluorescence. For example, a putative two-helix bundle peptoid (**10**; 30_Chi_CN_FQ) showed a FRET efficiency of 0.87 at native condition, which corresponds to a distance of 22 Å.

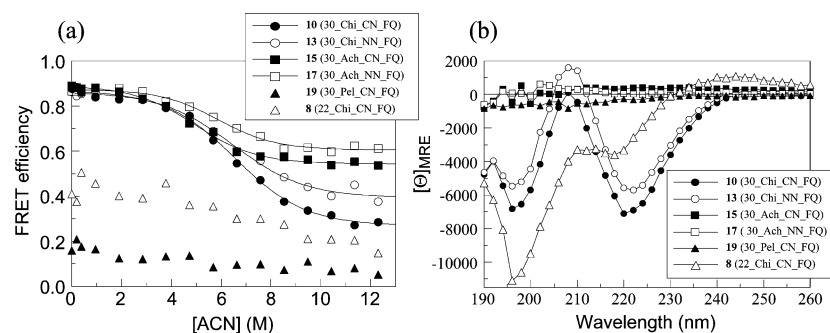


Figure 8. Equilibrium acetonitrile titration (a) and CD spectra (b) of each 30mer. CD spectra were measured at pH 7.0.

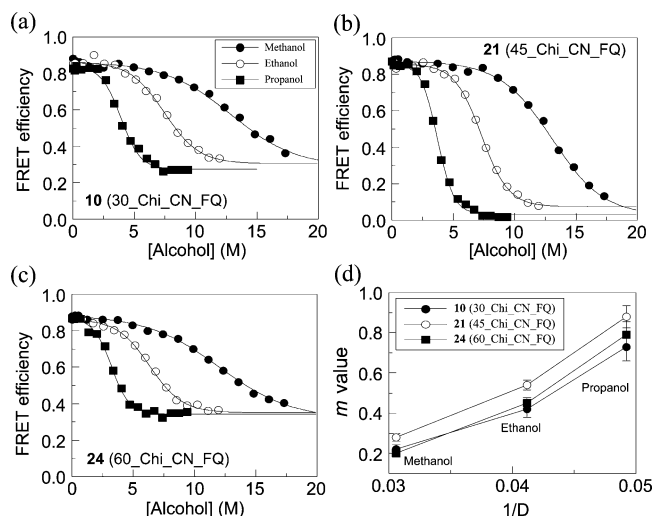


Figure 9. Equilibrium titration of peptoid helix bundles in a series of alcohols. (a) Peptoid **10** (30_Chi_CN_FQ), (b) peptoid **21** (45_Chi_CN_FQ), and (c) peptoid **24** (60_Chi_CN_FQ) were titrated with methanol (●), ethanol (○), and propanol (■). (d) The folding cooperativities of these peptoids are compared in terms of m value (in kcal/mol M^{-1}) and $1/D$, where D is the dielectric constant of each alcohol.

Circular dichroism (CD) spectra in the far-UV and near-UV regions (Figure 10d and e) were measured to see how the structural environments around amides and aromatic groups change respectively, upon varying the chain length. The structural environment around the backbone and side-chain amides changes when helical 15mer units are conjugated. However, further conjugations do not appear to affect the overall structure around the amides based on the amplitude of CD spectra at 220 nm (Figure 10d). Aromatic groups are positioned in different environments when the 15mers are conjugated.

Aromatic CD spectra in the near-UV region showed a blue shift in the maximum wavelength between the 15mer and the 60mer, and the amplitude of the CD signal changes at different chain lengths (Figure 10e). This could be interpreted as a structural rearrangement around the hydrophobic core, suggesting that the aromatic side-chains are accommodating their structures in the bigger helix bundle with a different geometry.

The length of the helical peptoid unit is calculated to be 22 Å because the FRET efficiency of the helical 15mer peptoid **5** (15_Chi_CN_FQ) is 0.87. End-to-end distance between helical units is also around 22 Å based on FRET efficiencies of peptoids **10** (30_Chi_CN_FQ), **21** (45_Chi_CN_FQ), and **24** (60_Chi_CN_FQ). The length of the helical peptoid unit is less than the expected value ($6 \text{ Å} \times 5 \text{ turns} = \sim 30 \text{ Å}$) where one helical pitch of peptoid is around 6 Å. This length of the helical pitch was obtained previously from the structural study of a penta-peptoid in organic solvents.^{17,18} So, the length of one helical pitch might be different in aqueous solution where hydrophobic interactions are stronger.

We synthesized a peptoid 45mer with a quencher positioned at the opposite end of the other helical unit with respect to the donor (**22**; 45_Chi_CN_FQ_2, Figure 11). When compared with the peptoid **21** (45_Chi_CN_FQ) where the quencher is located at the same side of other helical unit with respect to the donor, the FRET efficiency of the peptoid **22** (45_Chi_CN_FQ_2) is less than that of the peptoid **21** (45_Chi_CN_FQ) as expected from the molecular conformation of three-helix bundle (Figure 11). The profile of acetonitrile equilibrium titration of the peptoid **22** (45_Chi_CN_FQ_2) is the same as that of the peptoid **21** (45_Chi_CN_FQ) (Supporting Information). The molecular conformation of these peptoids could be roughly drawn using the information that we obtained here (Figure 11).

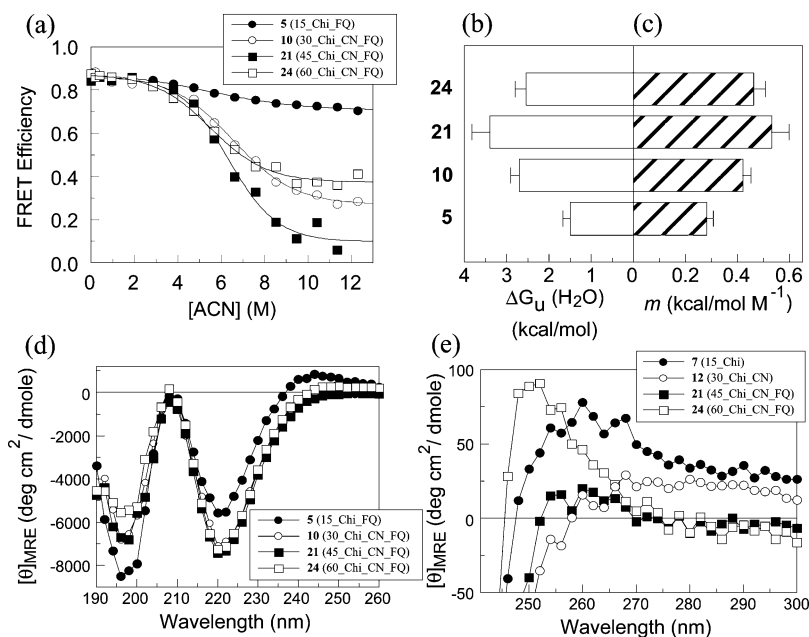


Figure 10. The effect of chain-length on folding cooperativity, stability, and structure. (a) Equilibrium acetonitrile titration of peptoids **5** (15_Chi_FQ), **10** (30_Chi_CN_FQ), **21** (45_Chi_CN_FQ), and **24** (60_Chi_CN_FQ). These peptoids are compared in terms of (b) stability and (c) folding cooperativity. (d) Far-UV CD spectra and (e) near-UV CD spectra of these peptoids are also compared. All CD spectra were obtained at native condition of pH 7 without denaturant. In near-UV CD spectra, peptoids **7** (15_Chi) and **12** (30_Chi_CN) without the fluorescent donor and quencher were used to remove the artifact of CD signal originated from the fluorescent donor and quencher.

Table 3. Thermodynamic Parameters of Each Peptoid Measured by Equilibrium Denaturation Titration^a

| | acetonitrile | | methanol | | ethanol | | 1-propanol | |
|--------------------------|---------------------------------|-------------|---------------------------------|-------------|---------------------------------|-------------|---------------------------------|-------------|
| | ΔG_u (H ₂ O) | m | ΔG_u (H ₂ O) | m | ΔG_u (H ₂ O) | m | ΔG_u (H ₂ O) | m |
| 5 (15_Chi_FQ) | 1.5 ± 0.2 | 0.28 ± 0.03 | | | | | | |
| 10 (30_Chi_CN_FQ) | 2.7 ± 0.2 | 0.42 ± 0.03 | 2.8 ± 0.2 | 0.22 ± 0.02 | 3.1 ± 0.3 | 0.42 ± 0.04 | 2.8 ± 0.3 | 0.73 ± 0.07 |
| 13 (30_Chi_NN_FQ) | 2.7 ± 0.3 | 0.41 ± 0.05 | | | | | | |
| 15 (30_Ach_CN_FQ) | 2.4 ± 0.2 | 0.48 ± 0.04 | 2.1 ± 0.5 | 0.18 ± 0.05 | 3.5 ± 0.2 | 0.53 ± 0.03 | 3.0 ± 0.3 | 0.83 ± 0.09 |
| 17 (30_Ach_NN_FQ) | 3.0 ± 0.4 | 0.51 ± 0.06 | | | | | | |
| 21 (45_Chi_CN_FQ) | 3.4 ± 0.4 | 0.53 ± 0.07 | 3.7 ± 0.2 | 0.28 ± 0.02 | 3.9 ± 0.2 | 0.54 ± 0.02 | 3.2 ± 0.2 | 0.88 ± 0.06 |
| 24 (60_Chi_CN_FQ) | 2.5 ± 0.3 | 0.46 ± 0.05 | 2.4 ± 0.1 | 0.20 ± 0.02 | 2.9 ± 0.2 | 0.45 ± 0.03 | 2.5 ± 0.2 | 0.79 ± 0.07 |

^a Units for ΔG_u (H₂O) and m are kcal/mol and kcal/mol M⁻¹, respectively.

Conclusions

In this work, we made progress toward the synthesis and characterization of a nonbiological single-chain sequence-specific heteropolymer with a tertiary structure. We synthesized helical bundles by covalently linking amphiphilic helical 15mer units into 30mers, 45mers, and 60mers, along with a fluorescent donor and quencher. To test for the formation of hydrophobic cores and FRET quenching between the ends of the chain, an indication of folding into a compact structure, we performed equilibrium denaturant titration. We found that several of these peptoids undergo cooperative transitions when titrated with acetonitrile and a series of alcohols, indicating that they have a stable hydrophobic core, resembling that of folded proteins. Because these denaturants do not disrupt the helical secondary structure, the observed transitions are the result of tertiary interactions between fully formed helices. Although our helix bundle molecules are compact, we have no evidence yet that they fold to unique native-like states, resembling those of proteins. Because of their ease of synthesis, high side-chain diversity, and protease resistance,²⁹ peptoids are a good platform

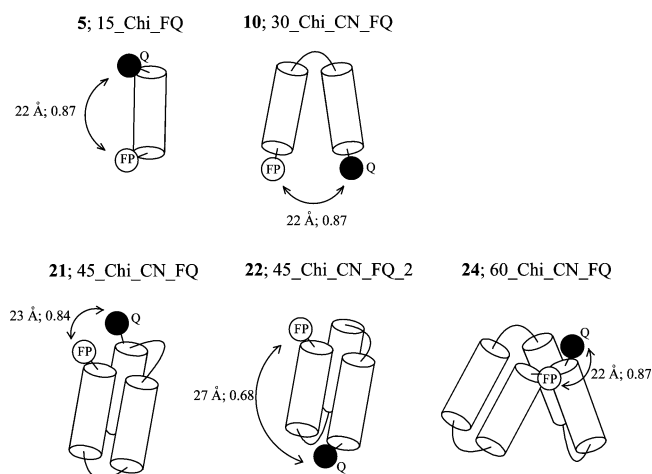


Figure 11. The schematic molecular conformations of putative helix bundle peptoids. In case of three-helix bundle, we synthesized two different peptoids where the fluorescence donor and quencher are positioned differently. When the quencher is incorporated into peptoid further apart from the donor (**22**; 45_Chi_CN_FQ_2), the FRET efficiency is lower than that of the peptoid **21** (45_Chi_CN_FQ). The calculated distance and FRET efficiency are shown at each putative helix bundle peptoid.

(29) Miller, S. M.; Simon, R. J.; Ng, S.; Zuckermann, R. N.; Kerr, J. M.; Moos, W. H. *Drug Dev. Res.* **1995**, *35*, 20–32.

to generate stable and active biomaterials. The ability to now generate compact folded structures opens up the possibility of introducing binding sites for specific molecular recognition and catalysis.

Experimental Section

Amine Submonomers for Peptoid Synthesis. Commercially available amines were purchased from Aldrich Chemical Co. (Milwaukee, WI), Fluka (Buchs, Switzerland), Acros Organics (Morris Plains, NJ), TCI America (Philadelphia, PA), and Bachem California, Inc. (Torrance, CA). See Table 1 for the chemical structure and abbreviations of side-chains used in our study.

(*S*)-*N*-(1-Phenylethyl) glycine (Nspe), (*S*)-*N*-(1-cyclohexylethyl) glycine (Nsch), *N*-(1-phenylmethyl) glycine (Npm), *N*-(1-cyclohexylmethyl) glycine (Nchm), *N*-(1-diphenylethyl) glycine (Ndpe), *N*-(2-carboxyethyl) glycine (Nglu), *N*-(methoxyethyl) glycine (Nme), and *N*-(2-nitrophenol) glycine (Nnp) were derived during peptoid synthesis from the amines L(-)- α -methylbenzylamine (Acros), *S*(+)-1-cyclohexylethylamine (Fluka), benzylamine (Aldrich), cyclohexylmethylamine (Aldrich), 2,2-diphenylethylamine (Aldrich), *tert*-butyl- β -alanine (Bachem), 2-methoxyethylamine (TCI America), and 4-amino-2-nitrophenol (Aldrich), respectively. (*S*)-*N*-(*N'*-2-Hydroxyethyl alaninamide) glycine (Nsahe), (*S*)-*N*-(*N'*-2-carboxyethyl alaninamide) glycine (Nsace), and (*S*)-*N*-(*N'*-2-aminoethyl alaninamide) glycine (Nsaae) with suitable protecting groups were synthesized as previously described.¹² *N*-(2-Hydroxyethyl) glycine (Nser) and *N*-(2-aminoethyl) glycine (Nae) were derived from [(triospropylsilyl)oxy]ethylamine and *N*-*t*-BOC-1,2-diaminoethane, which were prepared as described in elsewhere.^{30,31} *N*-(2-Anthranilamido-ethyl) glycine (Naae) was derived from 2-*tert*-butyloxycarbonylamino-1-aminoethyl-phenylamide that was made by coupling *N*-CBZ-ethylenediamine³² with 2-*tert*-butyloxycarbonylamino benzoate³² and removing the CBZ group by catalytic hydrogenation. The coupling reaction was the same as described previously.¹² All other solvents and reagents were obtained from commercial sources and used without further purification.

Peptoid Synthesis with N- and C-Terminal Modifications. The peptoid oligomers were synthesized on an automated peptoid/peptide robot synthesizer and purified as described previously with some modifications.¹⁴ Rink amide resin (0.57 mmol/g, Novabiochem, San Diego, CA) was used for peptoids to generate the C-terminal amide. Sasrin resin coupled with 2,2-dimethyl-1,3-dioxolane-4-methanamine (Supporting Information) and cysteamine 2-chlorotrityl resin (1.33 mmol/g, Novabiochem, San Diego, CA) were used for peptoids to generate the C-terminal aldehyde and sulfhydryl group, respectively. For N-terminal modification, aminoxyacetamide and 2-nitrophenylsulfenylmercaptoacetamide were incorporated into the peptoid N-terminus using previously described methods.²² These functional groups were used for chemoselective ligations between peptoids to form disulfide and oxime linkages.

Fmoc group on Rink amide resin was deprotected with 20% piperidine in DMF and washed with DMF five times before starting the submonomer cycle. Peptoid synthesis on 50 μ mol of resin was as follows: 1.2 M solution of bromoacetic acid in DMF (1.125 mL in DMF, 1.35 mmol) and 0.93 equiv of *N,N'*-diisopropylcarbodiimide (DIC) (0.2 mL, 1.25 mmol) were added to a resin-bound amine and mixed for 10 min at 35 °C during the acylation step of the submonomer cycle. After washing the resin with 2 mL of DMF five times, the resin-bound bromine was then displaced with the amine submonomer by adding a 1.5 or 2 M solution of the amine (0.85 mL) in *N*-methylpyrrolidinone (NMP). This displacement reaction was carried out for 40, 60, or 90 min at 35 °C, depending on the primary amine and the length of the peptoid. After the displacement reaction, the resin

was washed with 2 mL of DMF six times. In cases when Nnp and Naae were introduced at the first C-terminal residue, the displacement step was extended to 240 min for efficient coupling.

When alaninamide glycine derivative submonomers (Nsahe, Nsace, and Nsaae) were used in the peptoid, the molarity of bromoacetic acid in DMF was reduced to 0.4 M (0.45 mmol) with 67 μ L of DIC (0.45 mmol) after seven submonomers were added. In the displacement reaction, the incubation time of the first 10 displacement steps was 60 min, and the remaining five displacement steps were extended to 90 min.

In certain peptoids, aminoheptanoic acid was introduced at the C-terminus to give some flexibility for the peptoid ligation region. 0.4 M of Fmoc- ϵ Ahx-OH (Novabiochem, San Diego, CA) in DMF (0.8 mmol in 2 mL of DMF) was added to the resin-bound amine with 2 mL of 0.4 M hydroxybenzotriazole in DMF and 137 μ L of DIC (0.92 mmol). The reaction mixture was incubated at 35 °C for 120 min. Fmoc group was then deprotected with 20% piperidine in DMF for further peptoid synthesis. For the N-terminal modification, aminoxyacetamide and 2-nitrophenylsulfenylmercaptoacetamide were incorporated into the peptoid N-terminus as previously described.²²

Peptoid oligomers were cleaved from the resin with 95:5 trifluoroacetic acid (TFA)/water (v/v) for 50 min at room temperature with gentle stirring. The cleavage solution was filtered and evaporated under a stream of nitrogen to remove the TFA. The crude peptoid product dissolved in a mixture of water and acetonitrile was subjected to further purification by reverse-phase HPLC with a Vydac C4 column (10 μ m, 22 mm \times 250 mm). To generate the C-terminal aldehyde, the crude peptoid cleaved from the functionalized Sasrin resin was treated with 10 mL of 2 mM sodium periodate in 5:1 50 mM sodium phosphate buffer (pH 7.0):acetonitrile for 30 min to convert the C-terminal diol to the aldehyde. The reaction mixture was injected onto the HPLC to stop the reaction and purify the aldehyde product. To generate the C-terminal sulfhydryl group, the peptoid was cleaved from cysteamine 2-chlorotrityl resin with TFA (95:5 TFA/water (v/v)) and subjected to HPLC purification.

All reaction mixtures and final products were analyzed by analytical reverse-phase HPLC (5–95% gradient at 0.8 mL/min over 30 min at 60 °C with a C4 Duragel G C4, 5 μ m, 50 \times 2 mm column) and electrospray mass spectrometry (Hewlett-Packard Series 1100). The HPLC elution profile was monitored by the absorbance at 214 nm.

Ligation between Peptoids. HPLC-purified peptoid units were used directly for the ligation of peptoids. For the aldehyde-aminoxyacetamide ligation, peptoids were mixed in a 1:1 mixture with 0.1 M sodium acetate (pH 4.7). The reaction mixture was incubated for 1 h at room temperature and then subjected to purification by HPLC. For the disulfide ligation, the sulfhydryl and activated disulfide (2-nitrophenylsulfenylmercaptoacetamide) peptoids were mixed in a 1:1 mixture in 0.1 M sodium phosphate (pH 7.0) and the pH of the reaction mixture was further adjusted to 7.0 by adding a solution of sodium hydroxide. The reaction mixture was incubated for 1 h at room temperature and then subjected to purification by HPLC. Final peptoid oligomers were lyophilized, dissolved either in water or buffer (20 mM sodium phosphate, pH 7.0) and stored at -70 °C. Approximate peptoid concentrations were determined using the extinction coefficients of anthranilic acid ($\epsilon = 2000 \text{ M}^{-1} \text{ cm}^{-1}$ at 315 nm) and 2-nitrophenol ($\epsilon = 3500 \text{ M}^{-1} \text{ cm}^{-1}$ at 424 nm)²³ when they are incorporated into peptoids, otherwise peptoids were quantified by weight after lyophilization.

Fluorescence and Circular Dichroism Spectroscopy. Fluorescence from the anthranilamide side-chain (Naae) of the peptoids was measured at 25 °C with a fluorimeter (PTI photon technology international). The fluorescent probe was excited at 330 nm, and the emission was detected at 410 nm. Fluorescence emission was averaged for at least 10 s.

The effective distance (R_0) between the fluorescence donor (anthranilamide) and quencher (nitrophenol) can be obtained spectro-

(30) Zuckermann, R. N.; et al. *J. Med. Chem.* **1994**, *37*, 2678–2685.

(31) Krapcho, A. P.; Kuell, C. S. *Synth. Commun.* **1990**, *20*, 2559–2564.

(32) Atwell, G. J.; Denny, W. A. *Synthesis* **1984**, *12*, 1032–1033.

scopically by Förster fluorescence resonance energy transfer (FRET)³⁴ with the equation $R_0 = 9786(k^2n^{-4}Q_dJ)^{1/6}$. The 15mer peptoid **6** (15_Chi_F) was used for the measurement and calculation. The donor fluorescence quantum yield Q_d (0.57) was determined using quinine sulfate (0.55).³⁵ k and n are the relative orientation of the donor–quencher pair and the refractive index of the medium, respectively. k is assumed to be 2/3 for a random orientation. n is 1.4 in water. The overlap of the integral (J) was calculated to be $8.8 \times 10^{-15} \text{ M}^{-1} \text{ cm}^3$ from the overlap between the donor emission and quencher absorbance. A mathematical description of J can be found elsewhere.³⁴ With these parameters, R_0 is 31 Å. The actual distance (r) between the donor and quencher can be determined from the following equation: $r = R_0(E^{-1} - 1)^{1/6}$, where E is the FRET efficiency and is obtained from the quenching of donor fluorescence with $E = (1 - I_{da}/I_d)$, where I_{da} and I_d are the fluorescence intensities in the presence and absence of quencher, respectively. As a reference for measuring the FRET efficiency, analogous peptoids with only a donor, with no quencher, were also synthesized.

Circular dichroism (CD) measurements were carried out with a Jasco 710 spectropolarimeter at 25 °C. A 0.1 or 1 cm path length quartz cell was used for far-UV or near-UV CD, respectively. Step resolution, scan speed, response time, and bandwidth were 2 nm, 20 nm/min, 4 s, and 1.0 nm, respectively. All CD measurements were averaged with four scans. Fluorescence was measured at 2 μM of peptoids in 20 mM sodium phosphate buffer (pH 7.0) except when otherwise noted. CD was measured at 80 μM (15mer), 40 μM (30mer), 30 μM (45mer), and 20 μM (60mer) of peptoids in 20 mM sodium phosphate buffer (pH 7.0).

Equilibrium Denaturation Titration. To determine if there is a cooperative folding core, putative helix bundle peptoid oligomers were titrated with denaturants such as guanidine hydrochloride (GdnHCl), acetonitrile, and a series of alcohols (methanol, ethanol, and 1-propanol

at 25 °C). The data of denaturant-dependent FRET efficiency (E) were fitted by an apparent two-state transition from folded to unfolded state by the following equation.³⁶

$$E = \frac{a_n + a_u e^{(\Delta G_u(\text{H}_2\text{O}) - m[\text{D}])/RT}}{1 + e^{(\Delta G_u(\text{H}_2\text{O}) - m[\text{D}])/RT}}$$

where [D] is the denaturant concentration; a_n and a_u are the FRET efficiencies of folded and unfolded state extrapolated to zero denaturant; $\Delta G_u(\text{H}_2\text{O})$ is the free energy of unfolding in water; m is the denaturant dependence of free energy per mol of denaturant; R is the gas constant; and T is the temperature in Kelvin. Apparent $\Delta G_u(\text{H}_2\text{O})$ and m values can be obtained from the data fitting.

Acknowledgment. We thank Maria D. Calderon-Cacia and Dahzi Tang at Chiron Corp. for running several analytical gel filtrations and mass spectrometry, respectively. We also thank Thomas Horn, Tim Burkoth, Deb Charych, and Michael Connolly for valuable assistance.

Supporting Information Available: Complete citation for ref 30, method of coupling 2,2-dimethyl-1,3-dioxolane-4-methanamine into Sasrin resin, calculation of FRET efficiency, distance between the donor and quencher in peptoids used in our study, reaction profiles of peptoid ligations, equilibrium GdnHCl titration of peptoid helix bundles, concentration-dependence of equilibrium acetonitrile titration, analytical gel filtration of helix bundle peptoids, the effect of acetonitrile on the secondary structure of peptoid, and equilibrium denaturant titration of putative three-helix bundle 45mers with a quencher at different positions. This material is available free of charge via the Internet at <http://pubs.acs.org>.

(33) Meldal, M.; Breddam, K. *Anal. Biochem.* **1991**, *195*, 141–147.

(34) Lakowicz, J. R. *Principles of Fluorescence Spectroscopy*; Plenum Publishing Corp.: New York, 1983.

(35) Fletcher, A. N. *Photochem. Photobiol.* **1969**, *9*, 439–444.

JA0514904

(36) Santoro, M. M.; Bolen, D. W. *Biochemistry* **1988**, *27*, 8063–8068.